Electronic Supplementary Material (ESI) for Nanoscale.

Ultrastrong coupling of CdZnS/ZnS quantum dots to bonding breathing plasmons of aluminum metal-insulator-metal nanocavities in near-ultraviolet spectrum

Li Li,[1] Lei Wang,[2] Chenglin Du,[1] Zhongyuan Guan,[3] Yinxiao Xiang,[1] Wei Wu,[1] Mengxin Ren,[1,4,5] Xinzheng Zhang,[1,5] Aiwei Tang,[3] Wei Cai,[1,4,5,*] and Jingjun Xu[1,5,†]

[1] *The Key Laboratory of Weak-Light Nonlinear Photonics, Ministry of Education, School of Physics and TEDA Applied Physics Institute, Nankai University, Tianjin 300457, China*

[2] *College of Physics and Electronic Engineering, Xinyang Normal University, Xinyang 464000, China*

[3] *Key Laboratory of Luminescence and Optical Information, Ministry of Education, School of Science, Beijing Jiaotong University, Beijing 100044, China*

[4] *Renewable Energy Conversion and Storage Center, Nankai University, Tianjin 300071, China*

[5] *Collaborative Innovation Center of Extreme Optics, Shanxi University, Taiyuan, Shanxi 030006, People's Republic of China*

(Dated: November 29, 2019)

*Electronic address: weicai@nankai.edu.cn

†Electronic address: jjxu@nankai.edu.cn

I. OPTICAL PROPERTIES OF CdZnS/ZnS AND CuInZnSe/ZnS COLLOIDAL QUANTUM DOTS

The absorption spectrum of CdZnS/ZnS and CuInZnSe/ZnS colloidal quantum dots solution and cathodoluminescence (CL) spectrum of CdZnS/ZnS and CuInZnSe/ZnS colloidal quantum dots solution spin coated on Al film is shown in Figure S1. The emission peak of CdZnS/ZnS QDs is at 2.83 eV and has a line width of 0.19 eV. The emission peak of CuInZnSe/ZnS QDs is 2.01 eV.

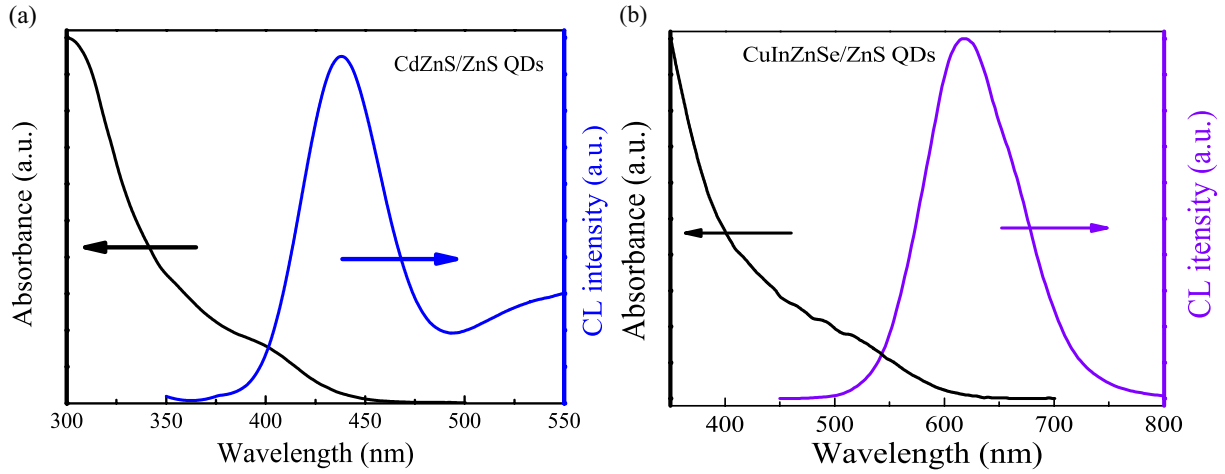

FIG. S1: (a) Absorbance spectrum of CdZnS/ZnS colloidal quantum dots solution and CL spectrum of a thin QDs CdZnS/ZnS QDs layer on Al film. (b)Absorbance spectrum of CuInZnSe/ZnS QDs colloidal quantum dots solution and CL spectrum of a thin QDs CdZnS/ZnS QDs layer on Al film

II. DIAMETER DISTRIBUTION DIAGRAM OF THE CdZnS/ZnS COLLOIDAL QDS ON ALUMINUM FILM

From the SEM image of the QDs distributed on aluminum film, we randomly selected 100 quantum dots and measured their diameters. The diameter distribution diagram of the CdZnS/ZnS QDs is shown in Figure S2. From the figure, we can find that the diameter of CdZnS/ZnS quantum dots is in the range 4.38± 0.76 nm.

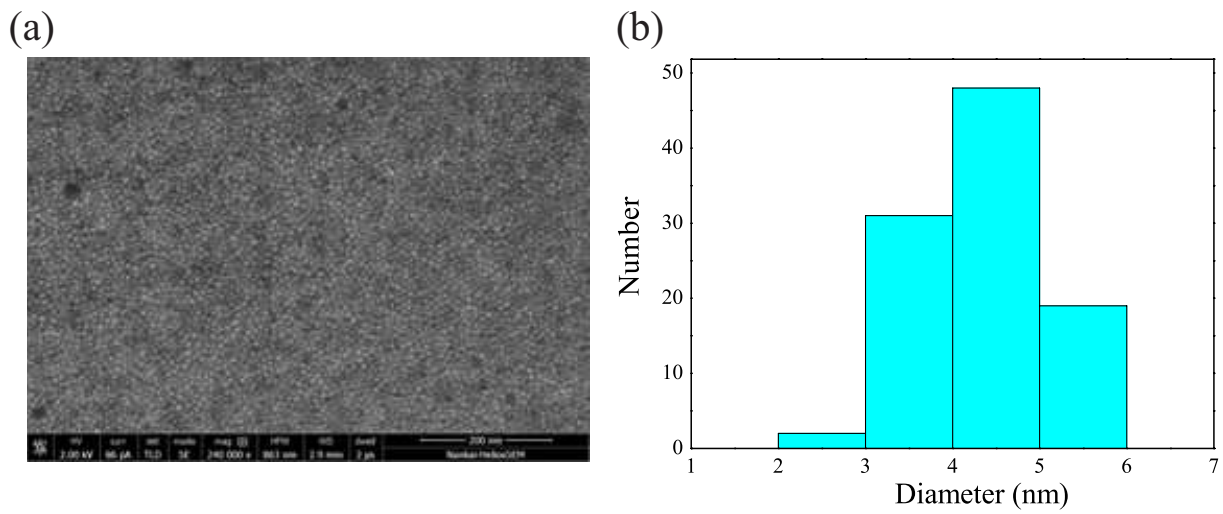

FIG. S2: Diameter distribution diagram of the CdZnS/ZnS quantum dots. (a) SEM image of the CdZnS/ZnS quantum dots spin coated on aluminum film. (b) Statistical diagram of the diameter distribution of 100 quantum dots.

III. CL SPECTRA OF CIRCULAR AL MIM CAVITIES LOADED WITH CdZnS/ZnS QDS AND CuInZnSe/ZnS QDS WITH DIFFERENT DISK DIAMETERS.

CL spectra of circular Al MIM cavities loaded with different volume radio of CdZnS/ZnS QDs and CuInZnSe/ZnS QDs was measured, by varying the diameter,D = 260nm, 280nm, 300nm, 320nm, the cavity resonance wavelenth to shift. Figures S3(a), (c), (e) and (g) corresponding to the CL spectra of the cavities loaded with the volume radio of CdZnS/ZnS QDs and CuInZnSe/ZnS QDs 1, $\frac{4}{5}$, $\frac{3}{5}$, $\frac{2}{5}$, $\frac{1}{5}$, respectively, with the gap thickness approximately 16nm. And we can obtain different rabbi spliting energy is 1.2 eV, 1 eV, 0.76 eV, 0.53 eV, 0.43 eV. Figures S3(b), (d), (f) and (h) corresponding to the simulated CL spectra of the MIM cavities with the same diameters as experiment,and fixed gap thickness g = 16 nm, the the reduced oscillator strength f = 0.2, 0.15, 0.09, 0.03, 0.02 in turn. There are some deviation between the experimental CL spectra and simulated CL spectra. The reason is in the experiment the thickness of QDs layer is not fixed 16nm, it is about $g = 16 \pm 6nm$.

IV. SIMULATED CL SPECTRA FOR THE METAL-INSULATOR-METAL (MIM) CIRCULAR CAVITIES WITH DIFFERENT GAP DISTANCES BETWEEN AL FILMS.

The plasmon response of circular Al MIM cavities across the emission energy of the uncoupled CdZnS/ZnS QDs by changing the gap distance g between the Al films was simulated. Figure S4(a) shows the dispersion of the MIM cavities for $g = 12, 14, 16, 18$ nm with $D = 290$ nm. One can find that the bonding breathing mode (0, 1) can couple with the excitons of the QDs, and the coupled CL intensity is shown in Figure S4 (b) when the QDs are loaded in MIM cavities. In contrast, if the gap distance $g = 6, 8, 10, 12$ nm for $D = 440$ nm, it is obvious that the bonding breathing plasmons (0, 2) is coupled with the excitons of the QDs (see Figure S5(a)-(b)). Peak energies of the plexcitonic complexes were then plotted as a function of detuning energies between plasmon resonance energy ω_p and the exciton energy ω_0. The dispersion curves are shown in Figures S4(c) and S5(c), it can be found that the coupling energy from the (0, 1) plasmon dispersion curve is approximately 1.2 eV while that from the (0, 2) plasmon dispersion curve is larger, approximately 1.25 eV, demonstrating that a larger Rabi splitting is induced by higher order plasmon modes.

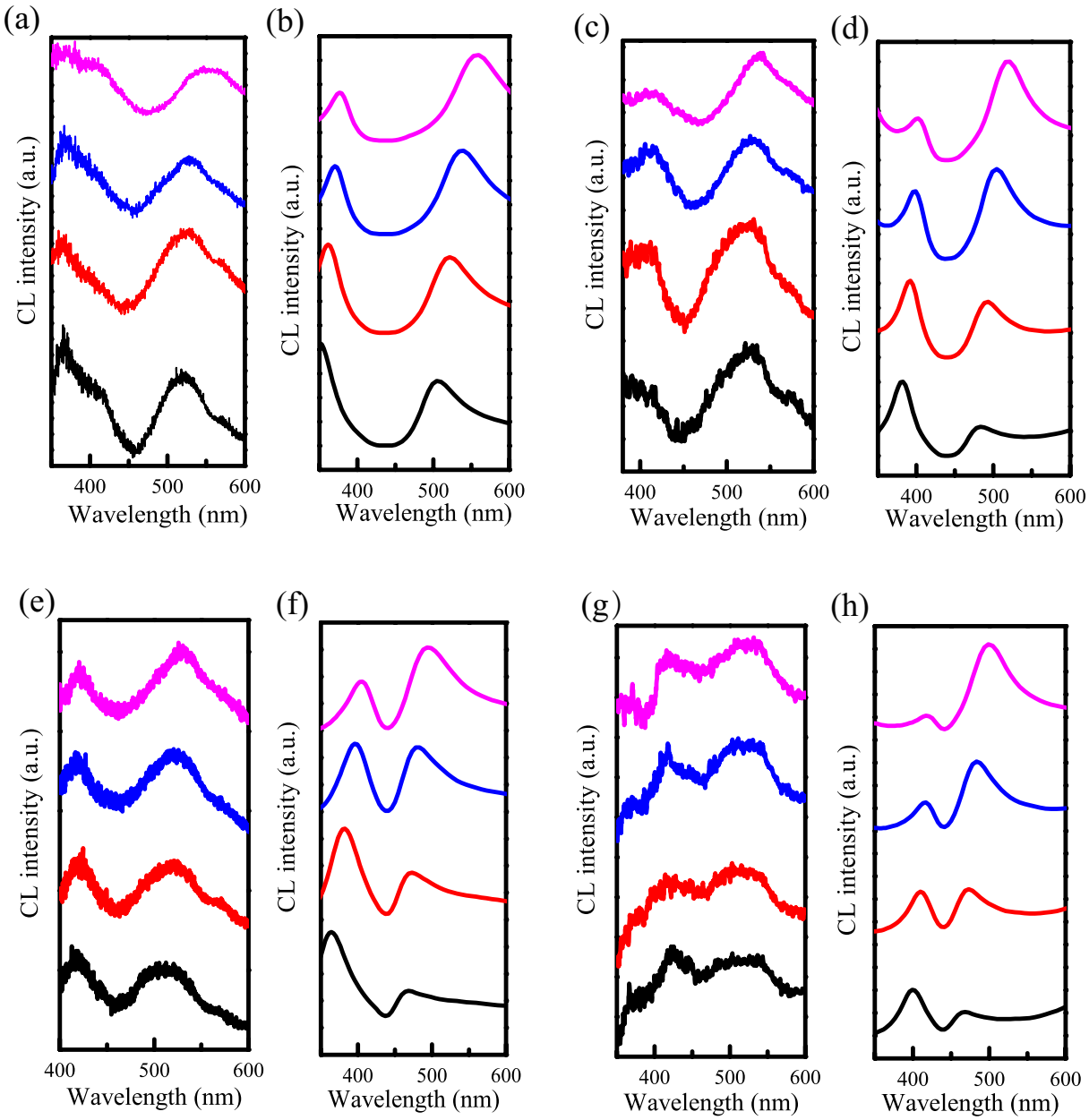

FIG. S3: (a), (c), (e) and (g) experimental CL spectra of circular Al MIM cavities loaded with the volume radio of CdZnS/ZnS QDs and CuInZnSe/ZnS QDs 1, $\frac{4}{5}$, $\frac{3}{5}$, $\frac{2}{5}$, $\frac{1}{5}$, respectively, with the varying diameter, D = 260nm, 280nm, 300nm, 320nm. The rabbi spliting energy is 1.2 eV, 1 eV, 0.76 eV, 0.53 eV, 0.43 eV, respectively for differenr volum radio. (b), (d), (f) and (h) simulated CL spectra of the MIM cavities with the same diameters as experiment, the reduced oscillator strength f = 0.2, 0.15, 0.09, 0.03, 0.02 in turn, and fixed gap thickness g = 16 nm.

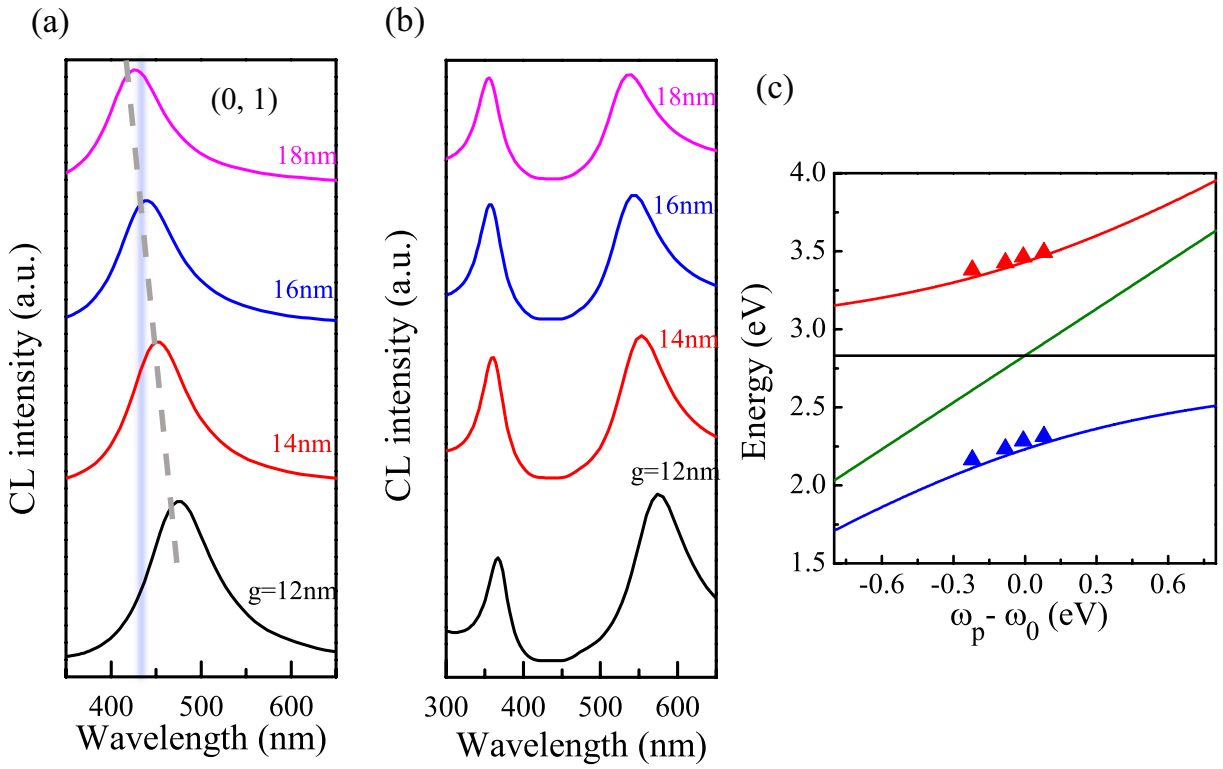

FIG. S4: (a) Simulated CL spectra of circular Al MIM cavities loaded with air with different gap distance g between the Al films, where the diameter of the disk is fixed at $D = 290$ nm. The mode evolutions of the selected peaks are indicated by the gray dashed lines, the blue shallow line indicates the position of the uncoupled exciton emission peak of CdZnS/ZnS QDs. (b) Simulated CL spectra of CdZnS/ZnS QDs sandwiched MIM plasmon cavities with different gap distance g between the Al film, and the diameter of the disk is chosen as $D = 290$ nm as well. (c) Dispersion curves from FDTD simulation (diamonds), theoretical fitting using a coupled oscillator model (solid lines). ω_p - ω_0 is the detuning between plasmon resonance energy ω_p and the exciton energy ω_0. The black and green lines represent uncoupled exciton and plasmon energies. Blue and red colors represent low and high energy plasmon-exciton hybrid states, respectively.

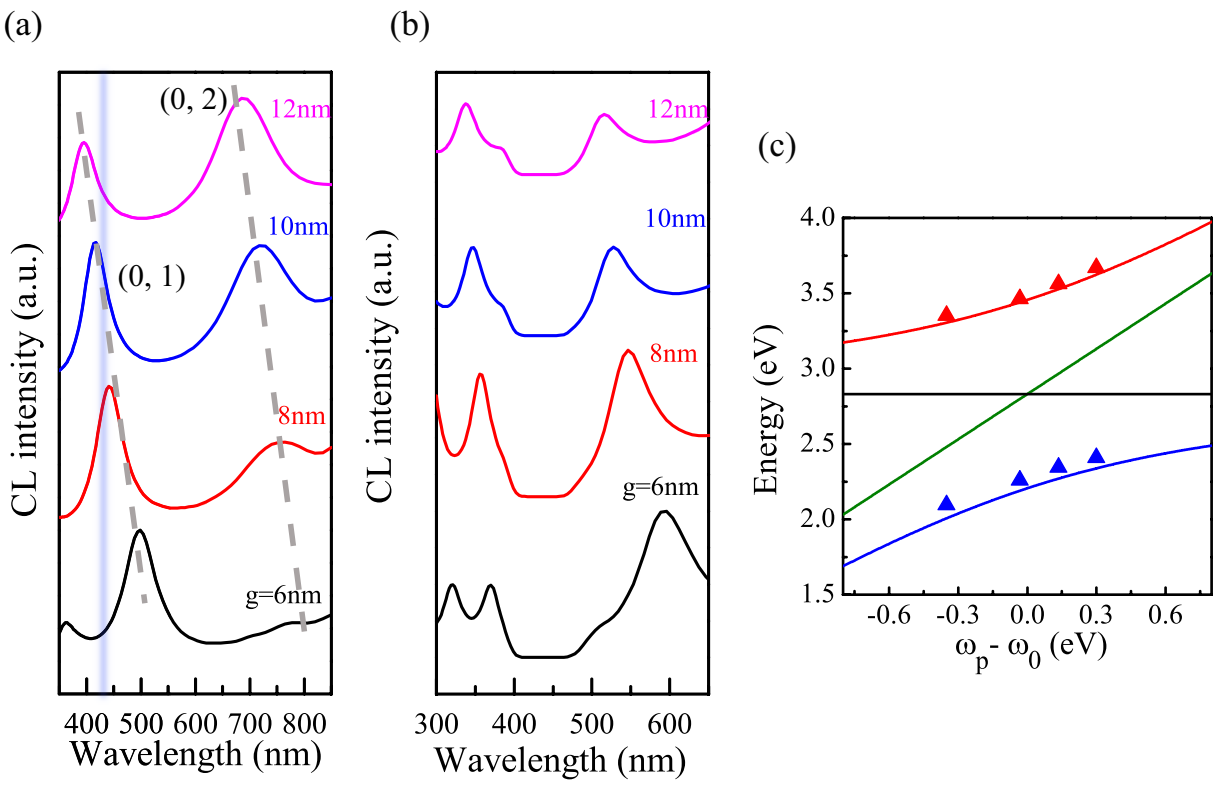

FIG. S5: (a) Simulated CL spectra of circular Al MIM cavities loaded with air with different gap distance g between the Al films, the diameter of the disk is chosen as $D = 440$ nm. The mode evolutions of the selected peaks are indicated by the gray dashed lines, the blue shallow line indicates the position of the uncoupled exciton emission peak of CdZnS/ZnS QDs. (b) Simulated CL spectra of CdZnS/ZnS QDs sandwiched MIM plasmon cavities with different gap distance g between the Al film with the diameter of the disk $D = 440$ nm. (c) Dispersion curves from FDTD simulation (diamonds), theoretical fitting using a coupled oscillator model (solid lines). ω_p - ω_0 is the detuning between plasmon resonance energy ω_p and the exciton energy ω_0. The black and green lines represent uncoupled exciton and plasmon energies. Blue and red colors represent low and high energy plasmon-exciton hybrid states, respectively.